Thermalization of a one-dimensional electron gas by many-body Coulomb scattering: Molecular-dynamics model for quantum wires

Martin Moško and Vladimír Cambel
Institute of Electrical Engineering, Slovak Academy of Sciences, Dúbravská cesta 9, SK-842 39 Bratislava, Slovak Republic
(Received 13 April 1994)

One-dimensional quantum-wire systems are peculiar in the sense that binary electron-electron collisions cannot thermalize the energy distribution of the electrons in the same subband. We show that such a thermalization occurs through many-body Coulomb scattering. We consider a one-dimensional electron gas described by Newton's equations of motion with many-body Coulomb forces. These equations are solved by the molecular-dynamics technique. Thermalization of the nonequilibrium distribution function towards Maxwell's function is demonstrated for a single-subband GaAs wire with electron density 1×10^5 cm^{-1}–3×10^5 cm^{-1} and electron temperature 200 K.

Recently, optical measurements[1,2] and Monte Carlo simulations[3,4] of one-dimensional carrier relaxation have been reported for GaAs quantum wires. It has been found that carrier relaxation is much slower than in bulk and two-dimensional systems under similar conditions. In particular, the electron cooling time due to polar-optic-phonon emission tends to increase with decreasing wire cross section and is as large as ~100 ps for a 100×100 Å^2 cross section.[4] Furthermore, it has been accepted that internal thermalization due to electron-electron scattering occurs only through intersubband binary collisions.[3,4] Intrasubband binary collisions cannot thermalize energy distribution of a one-dimensional electron gas.[3,4] This is indeed the case with the exception of some special cases. In the intrasubband binary collision an electron changes its momentum from k to k' by collision with another electron which is scattered from k_0 and k_0'. The screened matrix element of the Coulomb interaction between the electrons is[3]

$$M_{k,k_0\to k',k_0'}=\frac{e^2}{2\pi\epsilon_s L}\int dy\int dz\int dy'\int dz'\varphi^2(y,z)\varphi^2(y',z')\delta_{k+k_0,k'+k_0'+g}\frac{K_0(|k'-k|\sqrt{(y-y')^2+(z-z')^2})}{\epsilon(k'-k,(\varepsilon(k')-\varepsilon(k))/\hbar)}\ , \tag{1}$$

where $\varphi(y,z)$ is the electron envelope function in the considered subband (the x axis is assumed to be identical with the wire axis), L is the wire length, K_0 is the Bessel function, ϵ_s is the material permitivity, ϵ is the dielectric screening function, $\varepsilon(k)$ is the electron energy and g is the component (parallel with the wire axis) of a reciprocal lattice vector. The probability of the binary collision is given by Fermi's golden rule[5,6]

$$S_{k,k_0\to k',k_0'}=\frac{2\pi}{\hbar}[\tfrac{1}{2}|M_{k,k_0\to k',k_0'}-M_{k,k_0\to k_0',k'}|^2+\tfrac{1}{2}(|M_{k,k_0\to k',k_0'}|^2+|M_{k,k_0\to k_0',k'}|^2)]\times\delta(\varepsilon(k)+\varepsilon(k_0)-\varepsilon(k')-\varepsilon(k_0'))\ . \tag{2}$$

An inspection of (1) and (2) yields conservation of momentum and energy,

$$k+k_0-k'-k_0'=g,\quad \varepsilon(k)+\varepsilon(k_0)=\varepsilon(k')+\varepsilon(k_0')\ . \tag{3}$$

For $g=0$ and $\varepsilon(k)=\hbar^2k^2/2m$, where m is the electron effective mass, one gets $k'=k_0$ and $k_0'=k$. When the spins of the colliding electrons are parallel, there is no physical effect from such collision. When the spins are antiparallel, the only effect is the spin flip in states k and k_0. Since new momentum states cannot be created, intrasubband binary collisions do not thermalize the energy distribution.[3,4]

For $g=n2\pi/a$ (a is the lattice constant; $n=\pm1,\pm2,\ldots$) and $\varepsilon(k)=\hbar^2k^2/2m$ it is easy to see that $k'\neq k_0$ and $k_0'\neq k$. Such an umklapp process creates new momentum states, however, the probability of its realization is likely negligible (typical energies of the colliding electrons have to be of the order of 1 eV for $g=2\pi/a\approx10^{10}$ m^{-1}, while actual typical energies in GaAs wires are much lower).[1–4]

For $g=0$ and for nonparabolic dispersion $\varepsilon(1+\alpha\varepsilon)=\hbar^2k^2/2m$, where α is a constant, Eqs. (3) yield $k'\neq k_0$ and $k_0'\neq k$. Thus the thermalization through intrasubband binary collisions is possible, when the energy dispersion is nonparabolic. Up to now, to our knowledge, no estimations of this effect in real GaAs wires have been published.

There is, however, a more fundamental problem in the frame of the parabolic dispersion model. Fermi's golden rule (2) reduces the many-body Coulomb interaction to the binary collision processes, which cannot thermalize one-dimensional electrons in the same (parabolic) subband. Is such a thermalization prohibited also in the one-dimensional gas with many-body Coulomb interaction? In this work we show that many-body Coulomb collisions thermalize the nonequilibrium distribution to-

wards Maxwell distribution. For simplicity we examine many-body Coulomb kinetics of the classical one-dimensional electron gas. We use the molecular dynamics (MD) method to simulate the time development of the electron distribution in the GaAs quantum wire.

Similarly to Refs. 3 and 4 we analyze the electron dynamics, while the effect of holes is neglected. The perfectly one-dimensional electron gas with free motion in the x direction is assumed to occupy only the lowest-energy subband of the wire. The dynamics of an ith electron is governed by Newton equations $\dot{k}_i = F_i/\hbar$ and $\dot{x}_i = \hbar k_i/m$, where the Coulomb force is

$$F_i = \frac{e^2}{4\pi\epsilon_S} \sum_j \frac{(x_i - x_j)}{|x_i - x_j|^3} \tag{4}$$

with the summation over all other electrons. A similar classical formulation of many-body Coulomb kinetics has been used to study the electron transport in GaAs wires[7] as well as the relaxation of photoexcited carriers in two-dimensional[8] and three-dimensional[9] GaAs systems. Newton equations can be solved numerically without additional model approximations. Therefore, this MD approach avoids several approximations which cannot be avoided in Monte Carlo treatments of carrier-carrier scattering,[3-6] namely, the approximation of discrete binary collisions and the random-phase approximation for screening. In the MD approach "collisions" are treated as continuous many-body events and dynamic screening is automatically included.[9,10] Of course, MD is fully classical. Quantum corrections (exchange effects, Fermi statistics), included recently into the MD approach,[10] can be neglected in the nondegenerate limit of low carrier densities. We use our MD in this limit.

Equations $\dot{k}_i = F_i/\hbar$ and $\dot{x}_i = \hbar k_i/m$ are discretized as

$$k_i(t+\Delta t) = k_i(t) + \Delta t \frac{F_i(t)}{\hbar} , \tag{5}$$

$$x_i(t+\Delta t) = x_i(t) + \Delta t \frac{\hbar k_i(t+\Delta t)}{m} . \tag{6}$$

To simulate an infinitely large system using a finite number of particles, the following periodic boundary conditions are employed. We define a basic cell of the length L, that contains N electrons (typically $N = 1000$). When an electron leaves the cell crossing the boundary $x = L$, another electron is injected into the cell at the equivalent boundary $x = 0$ with the same k value. A similar procedure is used when an electron crosses the boundary $x = 0$. Thus an infinite system is simulated using finite and constant N.

Coulomb force (4) has to be recalculated after each time step Δt. To be consistent with the periodic boundary conditions an electron should be considered to interact with all other electrons in the cell and also will all electron images in the periodic replicas of the cell. This can be achieved through the Ewald sum method.[11] However, the implementation of the exact Ewald sum is too time consuming and often subject to numerical errors. In Ref. 12, a minimum image approximation for the Ewald sum has been found to work well for plasma coupling constant Γ as large as 36. [We note that $\Gamma = e^2/(4\pi\epsilon_S \lambda \bar{\epsilon})$, where λ is the mean interparticle distance and $\bar{\epsilon}$ is the mean kinetic energy of the electron.] In our case $\Gamma < 0.4$, i.e., the minimum image approximation should be even more reliable. In this approximation an electron is considered to interact only with $N-1$ electrons in the cell $\langle 0, L \rangle$ through specially defined interelectron distances. The calculated value of $x_i - x_j$ is used in the sum (4) only if $|x_i - x_j| \le L/2$. Otherwise the following replacement is used in (4). If $x_i - x_j > L/2$, then $x_i - x_j$ is replaced by $x_i - x_j - L$. If $x_i - x_j < -L/2$, then $x_i - x_j$ is replaced by $x_i - x_j + L$. Thus the particle at which the force is calculated sits at the center of its own cell.

Unfortunately, experience shows us that this approach is still too time consuming for our problem. Therefore we have also implemented a faster technique that truncates the Coulomb interaction for a pair of electrons with a distance greater than a cutoff length $R_C < L/2$. In this technique the sum (4) is modified using the same "minimum image" replacement for $|x_i - x_j| > L/2$ as described above. However, only terms with $|x_i - x_j| < R_C$ and terms with $|x_i - x_j \mp L| < R_C$ are taken into account in the summation. Of course, choosing $R_C = L/2$ one comes back to the minimum image approximation. The fast search for all electrons j within the distance R_C is performed according to the algorithm described in Ref. 13.

As in the minimum image approximation, also in the "truncation" technique the particle at which the force is calculated sits at the center of its own cell, but the length of the cell is $2R_C$, not L. Since $2R_C < L$, the number of interacting particles within the cell may change with time in the simulation process. This lowers the accuracy of the conservation of the total energy in the simulated ensemble. In the minimum image approximation there is no such problem, because an electron interacts during the simulation with the same number of partners. Nevertheless, in our situation (low Γ), above a certain R_C value the "truncation" technique gives results, which are independent on R_C and essentially the same as the results obtained by the minimum image approximation. In the same time the former approach provides one order of magnitude lower (three digit) accuracy of the conservation of total energy than the latter one, thus showing that the lower accuracy does not affect the results. Comparison of both techniques will be demonstrated later on. First we discuss the results obtained by the "truncation" technique.

Simulation parameters are $N = 1000$, $\Delta t = 0.1$ fs,[14] and $2R_C = 20/n_L$, where n_L is the linear electron density. Typically each electron interacts with 20 nearest partners. At the beginning of the simulation the initial k and x values are selected. The size of k is selected for each electron according to the Gaussian energy distribution of width 8.7 meV, centered at 8.7 meV. The sign of k is selected at random. Then x is selected at random in the cell $\langle 0, L \rangle$ with a supplementing condition that the generation of two electrons closer than 7 nm (for $n_L = 3\times10^5$ cm^{-1}), 8.5 nm (for $n_L = 2\times10^5$ cm^{-1}), and 10 nm (for $n_L = 1\times10^5$ cm^{-1}) is prohibited. This initiali-

zation, chosen by experience, ensures that during the simulation the mean kinetic energy remains the same as the initial mean energy ($\bar{\varepsilon}/k_B = 100$ K).

In Fig. 1 the occupation number versus energy and radial distribution[15] versus normalized distance are shown for times 0, 40 fs, . . . , 3 ps after the initialization. Simulation has been performed for $n_L = 3\times10^5$ cm^{-1}. The initial occupation number is strongly peaked as a result of the k selection from the Gaussian energy distribution. During the first picosecond one sees a fast relaxation of the occupation number towards the energy dependence which is still strongly non-Maxwellian. No remarkable change of this energy dependence is observed at times 1, 2, and 3 ps. Radial distribution also relaxes on subpicosecond time scale and remains unchanged at times > 500 fs. All the curves have been obtained by averaging the results of 30 simulations with a different ordering of random numbers used to initialize k and x. The curves from a single simulation would be more noisy.

Figure 2 shows how the occupation number from Fig. 1 progresses to relax at times 100, 200 ps,..., 10 ns. Figure 2 also shows the corresponding dependence on k. The occupation number converges towards equilibrium Maxwell function, shown in a dotted line for temperature 200 K. We note that curves in Fig. 2 are the time averages over 50-ps time intervals centered at shown times, rather than instantaneous ensemble averages at these times (such curves would be more noisy). This averaging process is appropriate, because there is almost no relaxation on a 50-ps time scale and changes due to noise occur on picosecond time scale.

On the nanosecond time scale of Fig. 2 the radial distribution (not shown) keeps the same shape as in Fig. 1 at times > 500 fs. In other words, the slow thermalization in Fig. 2 occurs in the regime of equilibrium radial distribution. The fast relaxation of the occupation number in Fig. 1 is closely related to the relaxation of the radial distribution. The increase of the radial distribution at distances close to zero is accompanied by the increase of the occupation number at energies close to zero. This is due to the fact that at $t = 0$ a part of electrons can have sufficiently high kinetic energies to move fast to very small mutual distances, where their motion is stopped by the increased repulsion. On the other hand, the increase

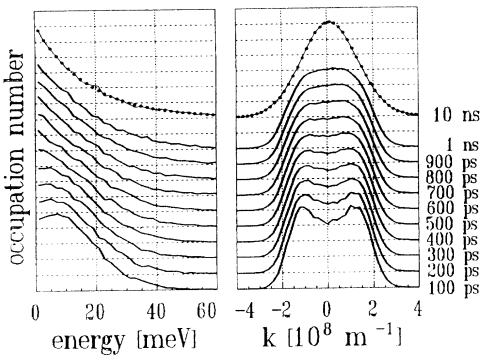

FIG. 2. Occupation number vs energy and k. This figure shows how the relaxation in Fig. 1 progresses at times 100, 200 ps, . . . , 10 ns. The occupation number converges towards equilibrium Maxwell function at temperature 200 K, shown in a dotted line. The spacing between horizontal grid lines is 0.05.

of the high-energy tail of the occupation number is due to the fact that at $t = 0$ there are some electron pairs which involve rather close partners with high kinetic energies and with different signs of their momenta. Repulsion of such partners further enhances their kinetic energies, thus creating the high-energy tail. Generally speaking, subpicosecond relaxation in Fig. 1 takes place because the initial momenta and initial positions are uncorrelated. We believe that during the fast relaxation the system searches for a stable correlation. For example, when two electrons become much closer than the mean interparticle distance, their kinetic energies should be typically much lower than the mean kinetic energy. Even this simple correlation is disregarded in the initialization of k and x. It should be mentioned that the fast thermalization is mainly due to the absence of correlations, rather than due to other details of the initialization. Test simulations show us that at times greater than 500 fs the curves in Fig. 1 remain (almost) unchanged when the initial positions are selected at equidistant x points and/or initial energies are selected from monoenergetic distribution. When the initial energies are selected from equilibrium Maxwell distribution, the occupation number remains in equilibrium, but radial distribution relaxes similarly to that in Fig. 1.

Spatiotemporal oscillations of the radial distribution in

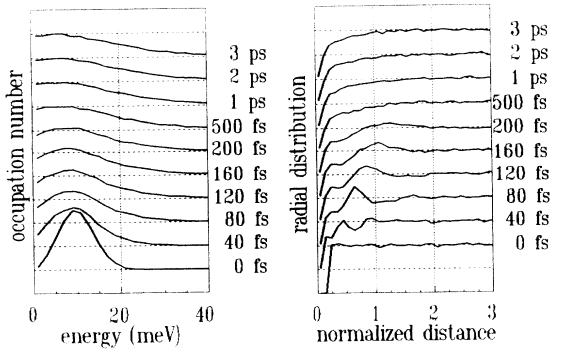

FIG. 1. Occupation number vs energy and radial distribution vs normalized distance d/n_L^{-1} for $n_L = 3\times10^5$ cm^{-1} at times 0, 40, 80 fs, . . . , 3 ps after the initialization. The spacing between horizontal grid lines is 0.25 and 0.5, respectively.

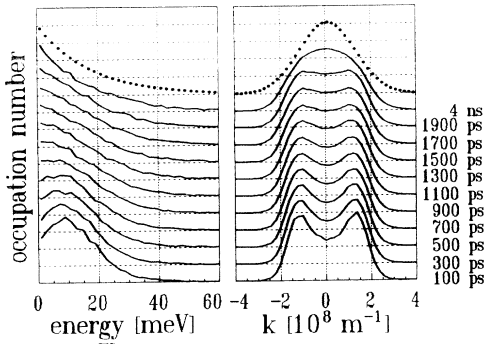

FIG. 3. Occupation number vs energy and k for $n_L = 2\times10^5$ cm^{-1} at times 100, 300 ps, . . . , 4 ns after the initialization. The spacing between horizontal grid lines is 0.05.

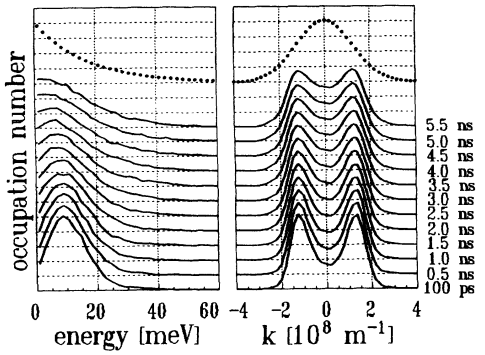

FIG. 4. Occupation number vs energy and k for $n_L = 1\times10^5$ cm^{-1} at times 100, 500 ps, . . . , 5.5 ns after the initialization. The spacing between horizontal grid lines is 0.025.

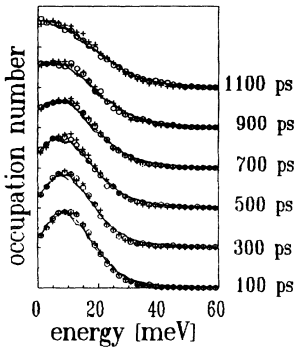

FIG. 5. Occupation number vs energy for $n_L = 2\times10^5$ cm^{-1}. Results of the "truncation" technique are shown in full lines ($N = 1000$, $2R_C = 20/n_L$), in dashed lines ($N = 1000$, $2R_C = 10/n_L$), and in open circles ($N = 200$, $2R_C = 20/n_L$). Results of the minimum image approximation for $N = 200$ are shown by crosses.

Fig. 1 at times 40–200 fs show that an electron efficiently affects the dynamics of several neighbors (and vice versa). Since the "reflections" of individual electrons in the ensemble are stochastic, oscillatory structure is damped fast. The equilibrium radial distribution within the nearest-neighbor distance is smaller than the transient radial distribution, i.e., close proximity ("collision") of several electrons is less probable. This provides qualitative understanding for the slow thermalization in Fig. 2, because it occurs in the regime of equilibrium radial distribution.

In Figs. 3 and 4 we show the same material as in Fig. 2, but for $n_L = 2\times10^5$ cm^{-1} and for $n_L = 1\times10^5$ cm^{-1}, respectively. One sees that with decreasing density the thermalization becomes much slower. We note that Figs. 3 and 4 show only the thermalization occurring in the regime of equilibrium radial distribution. The ultrafast relaxation during the first picosecond (not shown) is very similar to that presented in Fig. 1 for $n_L = 3\times10^5$ cm^{-1}. The only difference is that with decreasing n_L the equilibrated radial distribution becomes less different from the initial radial distribution and the occupation number becomes less relaxed (note that the occupation number in Figs. 3 and 4 has more pronounced peak at time 100 ps than the occupation number in Fig. 2).

All the calculations discussed up to now have been repeated using the minimum image approximation with $N = 200$. Due to long computing time, simulation time of 1200 ps has been chosen. In Fig. 5 we compare the "truncation" technique with the minimum image approximation for $n_L = 2\times10^5$ cm^{-1}. Except for the fluctuations no remarkable differences between both techniques are observed even in the case $2R_C = 10/n_L$, when an electron interacts only with the ten nearest partners in average. A similar agreement of both techniques has been found for $n_L = 3\times10^5$ cm^{-1} and $n_L = 1\times10^5$ cm^{-1}.

In conclusion, we have shown that *internal thermalization of the one-dimensional electron gas in a single-subband occurs through many-body Coulomb scattering.* Such a thermalization is not predicted by the Boltzmann H theorem.[16] The H theorem predicts the thermalization in a gas subjected to binary collisions but there is no thermalizing effect from such collisions in our one-dimensional case. Typical electron energies in our simulation are lower than optical phonon energy (36 meV). This situation could be realized experimentally by optical excitation of the carriers close to the band gap. Electron-phonon interactions, ignored in our present work, could be further suppressed using low lattice temperatures. In this situation internal thermalization through many-body Coulomb scattering could be a quite important and observable effect. Of course, interactions with phonons (and with holes) should be included in a more detailed analysis of such experiments.

[1]R. Cingolani *et al.*, Phys. Rev. Lett. **67**, 891 (1991).
[2]J. Christen *et al.*, Appl. Phys. Lett. **61**, 67 (1992).
[3]L. Rota *et al.*, Phys. Rev. B **47**, 1632 (1993).
[4]I. Vurgaftman and J. Singh, Appl. Phys. Lett. **62**, 2251 (1993).
[5]A. Mošková and M. Moško, Phys. Rev. B **49**, 7443 (1994).
[6]M. Moško and A. Mošková, Semicond. Sci. Technol. **9**, 478 (1994).
[7]K. Yano and D. K. Ferry, Phys. Rev. B **46**, 3865 (1992).
[8]V. Cambel and M. Moško, Semicond. Sci. Technol. **9**, 474 (1994).
[9]L. Rota *et al.*, Phys. Rev. B **47**, 4226 (1993).
[10]R. P. Joshi *et al.*, Appl. Phys. Lett. **58**, 2369 (1991).
[11]M. P. Allen and D. J. Tildsley, *Computer Simulation of Liquids* (Clarendon, Oxford, 1987).
[12]T. Yamada and D. K. Ferry, Phys. Rev. B **47**, 6416 (1993).
[13]V. Cambel and M. Moško, Semicond. Sci. Technol. **8**, 364 (1993).
[14]Due to the divergency of the pair Coulomb force at zero distance the integration scheme (5,6) can be numerically unstable. Therefore, if accidentally two electrons become closer than 1 nm, the force between them is approximated by its value at 1 nm. These infrequent events have negligible effect on final results [for a more detailed discussion see R. Hockney and J. Eastwood, *Computer Simulation Using Particles* (McGraw-Hill, New York, 1981)].
[15]Radial distribution is the probability (per unit distance) to find a particle at the distance d from another particle positioned at $d = 0$.
[16]E. M. Lifshits and L. P. Pitaevskii, *Physical Kinetics* (Pergamon, Oxford, 1982).